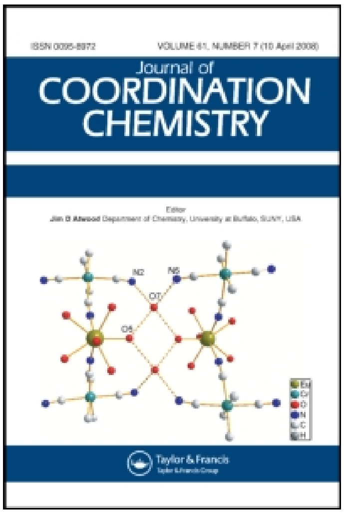

Journal of Coordination Chemistry
Publication details, including instructions for authors and subscription information:
http://www.informaworld.com/smpp/title~content=t713455674

Synthesis and characterization of two new inorganic-organic hybrid cobalt molybdenum(V) phosphates

Ying Ma[a]; YangGuang Li[a]; EnBo Wang[a]; Ying Lu[a]; XinLong Wang[a]; XinXin Xu[a]
[a] Department of Chemistry, Institute of Polyoxometalate Chemistry, Northeast Normal University, Changchun, P.R., China

To cite this Article Ma, Ying , Li, YangGuang , Wang, EnBo , Lu, Ying , Wang, XinLong and Xu, XinXin(2007) 'Synthesis and characterization of two new inorganic-organic hybrid cobalt molybdenum(V) phosphates', Journal of Coordination Chemistry, 60: 7, 719 — 732

To link to this Article: DOI: 10.1080/00958970600914705

URL: http://dx.doi.org/10.1080/00958970600914705

Journal of Coordination Chemistry
Vol. 60, No. 7, 10 May 2007, 719–732

Synthesis and characterization of two new inorganic–organic hybrid cobalt molybdenum(V) phosphates

YING MA, YANGGUANG LI, ENBO WANG*, YING LU, XINLONG WANG
and XINXIN XU

Department of Chemistry, Institute of Polyoxometalate Chemistry, Northeast Normal University, Changchun, 130024 P.R. China

(*Received 27 February 2006; in final form 5 May 2006*)

Two new inorganic–organic hybrid cobalt phosphomolybdates $(Hdien)_2[Co(dien)]_2[Co(dien)(H_2O)]_2[CoMo_{12}O_{24}(HPO_4)_2(H_2PO_4)_2(PO_4)_4(OH)_6]\cdot 5H_2O$ (**1**) and $(H_2dien)_2[Co(dien)]_2[Co(H_2O)_2]_2[CoMo_{12}O_{24}(HPO_4)_4(PO_4)_4(OH)_6]\cdot 7H_2O$ (**2**) (dien = diethylenetriamine), involving molybdenum in the V oxidation state and covalently bonded transition metal complexes, have been prepared under mild hydrothermal conditions and structurally characterized by elemental analyses, IR spectra, TG analyses, and single-crystal X-ray diffraction. Compound **1** exhibits a one-dimensional (1D) chain framework, in which dien molecules adopt two kinds of coordination modes. Compound **2** shows a two-dimensional (2D) layer framework with three types of unusual tunnels. To the best of our knowledge, it is the first time [Co(dien)] units are directly incorporated into 1D and 2D skeletons of reduced molybdenum phosphates. The electrochemical properties of the two compounds were studied *via* the method of bulk-modified carbon paste electrodes. Furthermore, the magnetic properties of compound **2** are reported.

Keywords: Inorganic–organic hybrid; Polyoxometalates; Hydrothermal synthesis; Crystal structure; Cobalt phosphomolybdates; Transition metal complexes

1. Introduction

In the past few years, considerable attention has been paid to inorganic–organic hybrid materials due to their rich structural chemistry and potential applications in fields such as catalysis, sorption, electrical conductivity and photochemistry [1]. With the development of hydrothermal techniques, a number of structurally complex solid state inorganic-organic materials have been prepared, including transition metal phosphates [2], zeolites [3], and vanadium oxides [4]. Polyoxometalates (POMs), as one kind of well-known metal oxide clusters with nanosizes and abundant topologies have

---

*Corresponding author. Email: wangenbo@public.cc.jl.cn

Journal of Coordination Chemistry
ISSN 0095-8972 print/ISSN 1029-0389 online
DOI: 10.1080/00958970600914705

recently been employed as inorganic building blocks for the construction of organic–inorganic hybrid materials [5]. These metal-oxide clusters are even more fascinating when they are modified by transition metal complexes, due to applications in interdisciplinary areas [6]. In the fields of POMs, reduced molybdenum phosphates have received attention for their wide applications in catalysis, ion exchange and molecular sieves [7]. Basic building units of $[Mo_6P_4]$ have frequently been reported with diverse structures ranging from one-dimensional (1D) polymers to three-dimensional (3D) microporous or tunnel materials [8]. In this work, $[Mo_6P_4]$ usually was modified by alkali metal or transition metal cations, with organic components or transition metal complexes presented as charge-compensating cations, such as $(NH_3CH_2CH_2NH_3)(NH_3CH_2CH_2NH_2)_3Na_3[Co_4Mo_{12}O_{24}(OH)_6(H_2O)_2(HPO_4)_2(PO_4)_6] \cdot 12H_2O$ [9], $(NH_3CH_2CH_2NH_3)Na[Ni_2Mo_{12}O_{30}(PO_4)(HPO_4)_4(H_2PO_4)_3] \cdot 6H_2O$ [10], $(C_4N_2H_{10})_5[Co_3Mo_{12}O_{18}(HOPO_3)_6(PO_4)_2(OH)_{12}(H_2O)_4] \cdot 9H_2O$ [11] and $[(C_{10}H_8N_2)_3Fe^{II}]_3Fe^{II}_2Fe^{III}_2Mo^{V}_{24}(H_2PO_4)_8(HPO_4)_4(PO_4)_4O_{48}(OH)_{12}(H_2O)_4 \cdot 12H_2O$ [12a]. However, examples with transition metal complexes covalently bonded to the $[Mo_6P_4]$ frameworks have rarely been reported [13].

We are interested in construction of novel molybdenum phosphates based on $[Mo_6P_4]$ units, using transition metal complexes as the bridging ligands. Here, we reported two new organic-inorganic hybrid cobalt phosphomolybdates $(Hdien)_2[Co(dien)]_2[Co(dien)(H_2O)]_2[CoMo_{12}O_{24}(HPO_4)_2(H_2PO_4)_2(PO_4)_4(OH)_6] \cdot 5H_2O$ (**1**) and $(H_2dien)_2[Co(dien)]_2[Co(H_2O)_2]_2[CoMo_{12}O_{24}(HPO_4)_4(PO_4)_4(OH)_6] \cdot 7H_2O$ (**2**) (dien = diethylenetriamine). Both compounds are based on $\{Co[Mo_6P_4]_2\}$ units, which are linked through [Co(dien)] complexes by corner sharing P–O–M (M = metal) units. Compound **1** exhibits a one-dimensional (1D) chain framework, in which dien molecules adopt two kinds of coordination modes. Compound **2** shows a two-dimensional (2D) layer framework with three types of unusual tunnels. To the best of our knowledge, these represent the first [Co(dien)] complex units directly incorporated into 1D and 2D skeletons of reduced molybdenum phosphates. The electrochemical properties of the two compounds are studied via the method of bulk-modified carbon paste electrodes and the magnetic properties of **2** are reported.

2. Experimental

2.1. *Materials and measurements*

All chemicals purchased were of reagent grade and used without further purification. Elemental analyses (C, H and N) were performed on a Perkin-Elmer 2400 CHN elemental analyzer. Mo, Co and P were determined by a Leaman inductively coupled plasma (ICP) spectrometer. FTIR spectra were recorded in the range 4000–400 cm^{-1} on an Alpha Centaurt FTIR spectrophotometer using KBr pellets. TG analyses were performed on a Perkin-Elmer TGA7 instrument in flowing N_2 with a heating rate of $10^\circ C\,min^{-1}$. The magnetic susceptibility data were measured with a Quantum Design SQUID magnetometer MPMS-XL in the temperature range of 2–300 K at 10,000 Oe.

2.2. *Hydrothermal synthesis*

Compounds **1** and **2** were hydrothermally synthesized under autogenous pressure. Compound **1** was prepared from MoO_3 (0.3 mmol), $CoCl_2 \cdot 6H_2O$ (0.6 mmol), dien (0.5 mL) and 7 mL of H_2O. The starting pH value was adjusted to 7.5 by the addition of H_3PO_4, and the mixture was stirred for 20 min in air. After that, the reagents were transferred to a Teflon-lined autoclave (20 mL) and kept at 160°C for five days. After slow cooling at a rate of $10^\circ C\,h^{-1}$ to room temperature, orange block-like crystals were filtered off with a small quantity of unidentifiable purple powder, washed with distilled water and dried in a desiccator at room temperature (yield: 30% based on Mo). The ICP analysis showed that compound **1** contained Mo, 33.40%; Co, 8.51%; P, 7.23% (Calcd: Mo, 33.42%; Co, 8.55%; P, 7.19%). The elemental analysis found: C, 8.39%; H, 3.14%; N, 7.30% (Calcd: C, 8.37%; H, 3.10%; N, 7.32%).

Compound **2** was synthesized by a similar procedure starting from a mixture of MoO_3 (0.3 mmol), $CoCl_2 \cdot 6H_2O$ (0.6 mmol), dien (0.5 mL) and 7 mL of H_2O. The starting pH value was adjusted to 6.0 by the addition of H_3PO_4, and the mixture was stirred for 20 min in air. After that, the reagents were transferred to a Teflon-lined autoclave (20 mL) and kept at 160°C for five days. After slow cooling at a rate of $10^\circ C\,h^{-1}$ to room temperature, dark-brown block-like crystals were filtered off together with a small quantity of unidentifiable purple powder, washed with distilled water and dried in a desiccator at room temperature (yield: 55% based on Mo). The ICP analysis showed that compound **2** contained Mo, 34.72%; Co, 8.87%; P, 7.50% (Calcd: Mo, 34.77%; Co, 8.90%; P, 7.48%). The elemental analysis found: C, 5.82%; H, 2.71%; N, 5.04% (Calcd: C, 5.80%; H, 2.68%; N, 5.08%).

2.3. *X-ray crystallography*

The structures of **1** and **2** were determined by single crystal X-ray diffraction. An orange single crystal of **1** with dimensions $0.33 \times 0.28 \times 0.25\,mm^3$ was glued on a glass fiber. Data were collected on a Rigaku *R*-axis RAPID IP diffractometer at 293 K using graphite-monochromated Mo-Kα radiation ($\lambda = 0.71073$ Å) and IP technique in the range of $2.15^\circ < \theta < 25.00^\circ$. Empirical absorption corrections were applied.

A dark-brown single crystal of **2** with dimensions $0.30 \times 0.26 \times 0.24\,mm^3$ was glued on a glass fiber. Data were collected on a Rigaku *R*-axis RAPID IP diffractometer at 293 K using graphite-monochromated Mo-Kα radiation ($\lambda = 0.71073$ Å) and IP technique in the range of $2.06^\circ < \theta < 25.00^\circ$. Empirical absorption corrections were applied.

The structures of **1** and **2** were solved by direct methods and refined by the full-matrix least-squares method on F^2 using the SHELXTL 97 crystallographic software package [14]. Anisotropic thermal parameters were used to refine all non-hydrogen atoms in **1** and **2**. In **1** and **2**, the hydrogen atoms attached to carbon atoms and nitrogen atoms were fixed in ideal positions and other hydrogen atoms were located from difference Fourier maps. Further details of the X-ray structural analysis for **1** and **2** are given in table 1. Selected bond lengths and angles of **1** and **2** are listed in tables 2 and 3, respectively. Crystal data and structure refinement, bond lengths and angles, and anisotropic displacement parameters were available in supplementary crystallographic data at CCDC.

Table 1. Crystal data and structure refinement for **1** and **2**.

	1	**2**
Empirical formula	$C_{24}H_{106}Co_5Mo_{12}N_{18}O_{69}P_8$	$C_{16}H_{88}Co_5Mo_{12}N_{12}O_{73}P_8$
Fw	3444.96	3310.67
Crystal system	Triclinic	Triclinic
Space group	$P\bar{1}$	$P\bar{1}$
a (Å)	12.935(3)	12.749(3)
b (Å)	13.372(3)	13.634(3)
c (Å)	14.384(3)	14.221(3)
α (°)	78.62(3)	74.76(3)
β (°)	89.81(3)	74.61(3)
γ (°)	68.15(3)	64.44(3)
V (Å^3)	2257.2(8)	2118.5(7)
Z	1	1
μ (mm^{-1})	2.759	2.935
T (K)	293(2)	293(2)
λ (Å)	0.71073	0.71073
Final R_1, wR_2 [$I > 2\sigma(I)$]	0.0492, 0.0891	0.0815, 0.1521
Final R_1, wR_2 (all data)	0.0657, 0.0938	0.1133, 0.1627
Largest diff. peak and hole (e A^{-3})	1.116 and −0.702	1.138 and −1.166

$R_1 = \Sigma\|F_o| - |F_c\|/\Sigma|F_o|$; $wR_2 = \Sigma[w(F_o^2 - F_c^2)^2]/\Sigma[w(F_o^2)^2]^{1/2}$.

3. Results and discussion

3.1. *Synthesis*

The molybdenum phosphates **1** and **2** are synthesized in similar reactions, starting from a slurry containing MoO_3, $CoCl_2 \cdot 6H_2O$, dien and H_3PO_4. In the process of hydrothermal synthesis, many factors can affect the formation and crystal growth of products, such as the type of initial reactants, molar ratio, pH value, reaction time and temperature. In this case, the initial pH value of the reaction system permits the connectivity of the $[Mo_6P_4]$ clusters and the cobalt ions, and hence the dimensionality of the framework. Indeed, compound **1** only forms in a limited pH range (7.5–8), as does compound **2** (6–6.5). Thus, the amounts of H_3PO_4 used should be carefully controlled because it acts both as a reactant and pH adjustor.

3.2. *Structure description*

Single crystal X-ray structural analysis shows that the basic building unit in **1** and **2** is $[Mo_6P_4]$, which is a classic metal oxide cluster, described by Haushalter [15]. As shown in figure 1(a), $[Mo_6P_4]$ is made up of six MoO_6 octahedra and four PO_4 tetrahedra. Each $[MoO_6]$ unit has a terminal oxygen atom and shares two edges with neighboring $[MoO_6]$ octahedra. Six $[MoO_6]$ octahedra are coplanar and constitute a hexameric molybdenum cluster with alternating Mo–Mo (av. 2.59 Å for **1**, 2.60 Å for **2**) bonds and non-bonding Mo–Mo contacts (av. 3.49 Å for **1**, 3.48 Å for **2**). The central PO_4 group provides three oxygen atoms that bridge the bonding Mo–Mo contacts, while each of the remaining three PO_4 groups has two oxygen atoms to span the non-bonding Mo–Mo contacts. The P–O bond length is in the range of 1.486(6) to 1.579(6) Å for **1**, 1.501(9) to 1.570(11) Å for **2.** Valence bond calculations [16] not only confirm that all Mo atoms are in reduced oxidation state (+5) and Co atoms are +2, but also show the

Table 2. Selected bond lengths (Å) for **1**.

Mo1–O27	1.686(5)	Mo1–O15	1.921(5)
Mo1–O10	1.966(5)	Mo1–O18	2.092(5)
Mo1–O1	2.094(5)	Mo1–O7	2.260(5)
Mo1–Mo6	2.579(1)	Mo2–O12	1.679(5)
Mo2–O16	1.936(5)	Mo2–O2	1.981(5)
Mo2–O21	2.069(5)	Mo2–O18	2.102(5)
Mo2–O7	2.299(5)	Mo2–Mo3	2.593(1)
Mo3–O14	1.674(5)	Mo3–O16	1.948(5)
Mo3–O2	1.991(5)	Mo3–O25	2.050(5)
Mo3–O20	2.103(5)	Mo3–O29	2.268(5)
Mo4–O24	1.692(5)	Mo4–O6	1.942(5)
Mo4–O19#1	1.992(5)	Mo4–O28	2.059(5)
Mo4–O20	2.100(5)	Mo4–O29	2.243(5)
Mo4–Mo5	2.598(1)	Mo5–O4	1.680(5)
Mo5–O6	1.940(5)	Mo5–O19#1	1.982(5)
Mo5–O17	2.045(5)	Mo5–O13	2.092(5)
Mo5–O22	2.288(5)	Mo6–O5	1.679(5)
Mo6–O15	1.945(5)	Mo6–O10	1.987(5)
Mo6–O11	2.045(5)	Mo6–O13	2.123(5)
Mo6–O22	2.260(5)	Co1–O2#1	2.159(5)
Co1–O2	2.159(5)	Co1–O19#1	2.159(5)
Co1–O19	2.159(5)	Co1–O10	2.169(5)
Co1–O10#1	2.169(5)	Co2–O30	2.003(5)
Co2–O9	2.029(5)	Co2–O#2	2.052(6)
Co2–N5	2.053(7)	Co2–N6	2.293(7)
Co3–O8	1.979(5)	Co3–N3	2.086(8)
Co3–N1	2.103(8)	Co3–O1W	2.117(5)
Co3–N2	2.191(7)	P1–O26	1.486(6)
P1–O21	1.524(6)	P1–O31	1.541(6)
P1–O23	1.579(6)	P2–O8	1.525(5)
P2–O9	1.525(5)	P2–O17	1.543(5)
P2–O11	1.546(5)	P3–O30#2	1.503(5)
P3–O22	1.538(5)	P3–O29	1.549(5)
P3–O7	1.549(5)	P4–O3	1.511(6)
P4–O1	1.530(6)	P4–O28	1.556(5)
P4–O25	1.558(6)		

Symmetry transformations used to generate equivalent atoms, #1: $-x$, $-y$, $-z$; #2: $-x$, $-y$, $-z+1$.

μ_2-O atoms between non-bonding Mo atoms (O13, O18, O20 for **1**, O27, O28, O31 for **2**) and part of P–O groups (O3, O23, O26 for **1**, O2, O10 for **2**) are protonated. The molybdenum hexamer thus can be formulated as $[Mo_6O_{12}(H_2PO_4)(HPO_4)(PO_4)(OH)_3]^{6-}$ for **1** and $[Mo_6O_{12}(HPO_4)_2(PO_4)_2(OH)_3]^{7-}$ for **2**. In both **1** and **2**, a Co^{2+} is a regular octahedral coordination and bridges two $[Mo_6P_4]$ units into a dimer via three μ_3-O's to give the $Co[Mo_6P_4]_2$ units, as shown in figure 1(b).

The structure of **1** is constructed from $Co[Mo_6P_4]_2$ dimers bonded together with square-pyramidal Co^{2+} into a 1D chain. It is interesting that there are three distinct cobalt coordination environments in compound **1** (shown in figure 2a). One (Co1) is located in the $Co[Mo_6P_4]_2$ dimers and displays octahedral CoO_6 coordination geometry as mentioned above, while the remaining two (Co2 and Co3) exhibit square-pyramidal CoN_2O_3 and CoN_3O_2 coordination, respectively. Obviously, the coordination modes of dien with Co2 and Co3 are entirely different. One is bidentate chelate through two nitrogen atoms (N5 and N6) with Co2, while the other displays tridentate chelate coordination through three nitrogen atoms (N1, N2 and N3) with Co3. Besides the different coordination mode with dien molecules, another difference between Co2 and

Table 3. Selected bond lengths (Å) for **2**.

Mo1–O20	1.675(1)	Mo1–O29	1.945(9)
Mo1–O30	1.968(8)	Mo1–O24	2.048(9)
Mo1–O31	2.091(9)	Mo1–O13	2.304(9)
Mo1–Mo2	2.595(2)	Mo2–O9	1.669(9)
Mo2–O29	1.944(9)	Mo2–O30	1.984(9)
Mo2–O22	2.033(9)	Mo2–O28	2.106(9)
Mo2–O17	2.293(9)	Mo3–O1	1.671(9)
Mo3–O25	1.955(9)	Mo3–O23	1.975(9)
Mo3–O21	2.059(9)	Mo3–O31	2.080(8)
Mo3–O13	2.315(9)	Mo3–Mo4	2.603(2)
Mo4–O18	1.677(1)	Mo4–O25	1.943(9)
Mo4–O23	2.007(9)	Mo4–O7	2.057(1)
Mo4–O27	2.104(9)	Mo4–O19	2.263(9)
Mo5–O11	1.681(9)	Mo5–O15	1.941(9)
Mo5–O26	1.977(9)	Mo5–O16	2.061(1)
Mo5–O27	2.084(9)	Mo5–O19	2.230(8)
Mo5–Mo6	2.594(2)	Mo6–O12	1.677(9)
Mo6–O15	1.949(9)	Mo6–O26	1.992(9)
Mo6–O14	2.071(9)	Mo6–O28	2.094(9)
Mo6–O17	2.241(9)	Co1–O30	2.136(8)
Co1–O30#1	2.136(8)	Co1–O26#1	2.151(9)
Co1–O26	2.151(9)	Co1–O23	2.183(9)
Co1–O23#1	2.183(9)	Co2–O3	2.031(1)
Co2–O6#2	2.039(1)	Co2–N3	2.073(1)
Co2–N1	2.097(1)	Co2–N2	2.202(2)
Co3–O8	1.982(1)	Co3–O7W	2.021(1)
Co3–O4	2.036(9)	Co3–O5	2.055(1)
Co3–O6W	2.200(1)	P1–O2	1.520(1)
P1–O7	1.531(1)	P1–O8	1.540(1)
P1–O16	1.570(1)	P2–O10	1.513(9)
P2–O3	1.533(1)	P2–O14	1.538(1)
P2–O22	1.542(1)	P3–O6	1.515(1)
P3–O5#3	1.529(1)	P3–O21	1.543(9)
P3–O24	1.546(9)	P4–O4	1.501(9)
P4–O13	1.543(9)	P4–O17	1.548(9)
P4–O19	1.555(9)		

Symmetry transformations used to generate equivalent atoms, #1: $-x, -y+1, -z+1$; #2: $x+1, y, z$; #3: $-x, -y+1, -z$.

Co3 lies in that Co3 only bridges one P–O group (O8) in $[Mo_6P_4]$ and has a terminal water molecular (O1W), while Co2 is coordinated with two oxygen atoms (O9 and O30) from one $[Mo_6P_4]$ and a oxygen atom (O1) from the other $[Mo_6P_4]$ unit, thus completing their square-pyramidal coordination environment. The way Co2 and Co3 atoms bridge the end of the $Co[Mo_6P_4]_2$ dimer to form the 1D chain is shown in figure 2(b). In order to satisfy the electroneutrality of compound **1**, the free dien molecule has to be singly protonated.

In compound **2**, the $Co[Mo_6P_4]_2$ units are connected by square-pyramidal Co^{2+} into a 2D framework (see figure 3b). There are also three crystallographically independent Co atoms in **2** (shown in figure 3a). One (Co1), the same as compound **1**, is located in the $Co[Mo_6P_4]_2$ dimers and adopts octahedral coordination geometry. Co2 displays square-pyramidal geometry and links two P–O groups (O3 and O6) from two different $[Mo_6P_4]$ units, thus bridging $Co[Mo_6P_4]_2$ dimers together to exhibit a 1D chain. The remaining sites of Co2 are occupied by three nitrogen atoms (N1, N2 and N3) of a dien molecule to form [Co(dien)] fragments. Co3 links two adjacent chains to form an extended layer framework through coordinating with

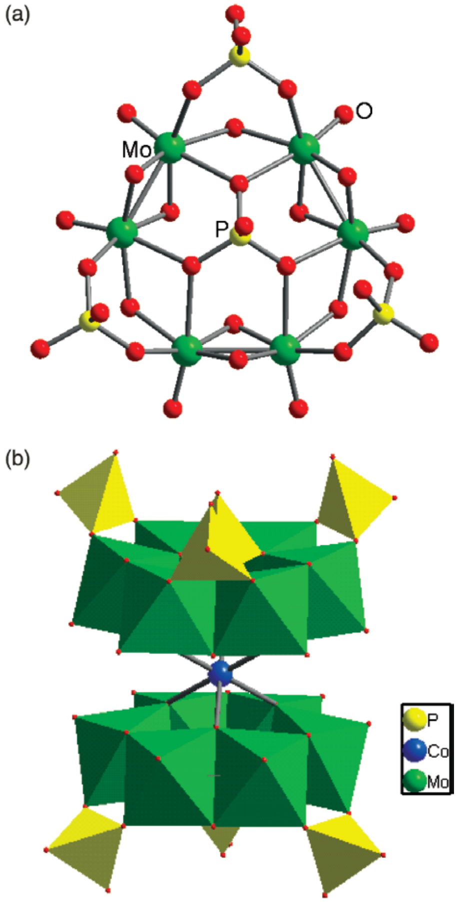

Figure 1. (a) Ball-stick representation of the basic building block [Mo_6P_4]. (b) View of the dimeric unit Co[Mo_6P_4]$_2$.

three μ_2-O atoms (O4, O5 and O8). Two terminal water molecules (O6W and O7W) complete the coordination sphere of Co3. Interestingly, three types of tunnels are formed in the solid of **2**, which can be labeled as A, B and C, respectively (see figure 3b). Tunnel A is formed by two [Co(dien)] units and two Co[Mo_6P_4]$_2$ dimers. Tunnel B is surrounded by two [Co(dien)] units, two Co coordination square-pyramids and six P–O tetrahedra. Tunnel C is constructed from two Co coordination square-pyramids and four P–O tetrahedra. The tunnels are filled with water molecules and dien ions. To our knowledge, such tunnels coexisting in the 2D layer which consists of [Mo_6P_4] and transition metals have not been reported.

It is noteworthy that not only transition metal cations are coordinated with the inorganic groups [Mo_6P_4], but also the organic amine molecules are incorporated into the 1D and 2D framework of **1** and **2**. In addition, the cobalt cations in compounds **1** and **2** exhibit both square-pyramidal and octahedral coordination different from that of cobalt molybdenum phosphates containing M[Mo_6P_4]$_2$ as building blocks [7–12].

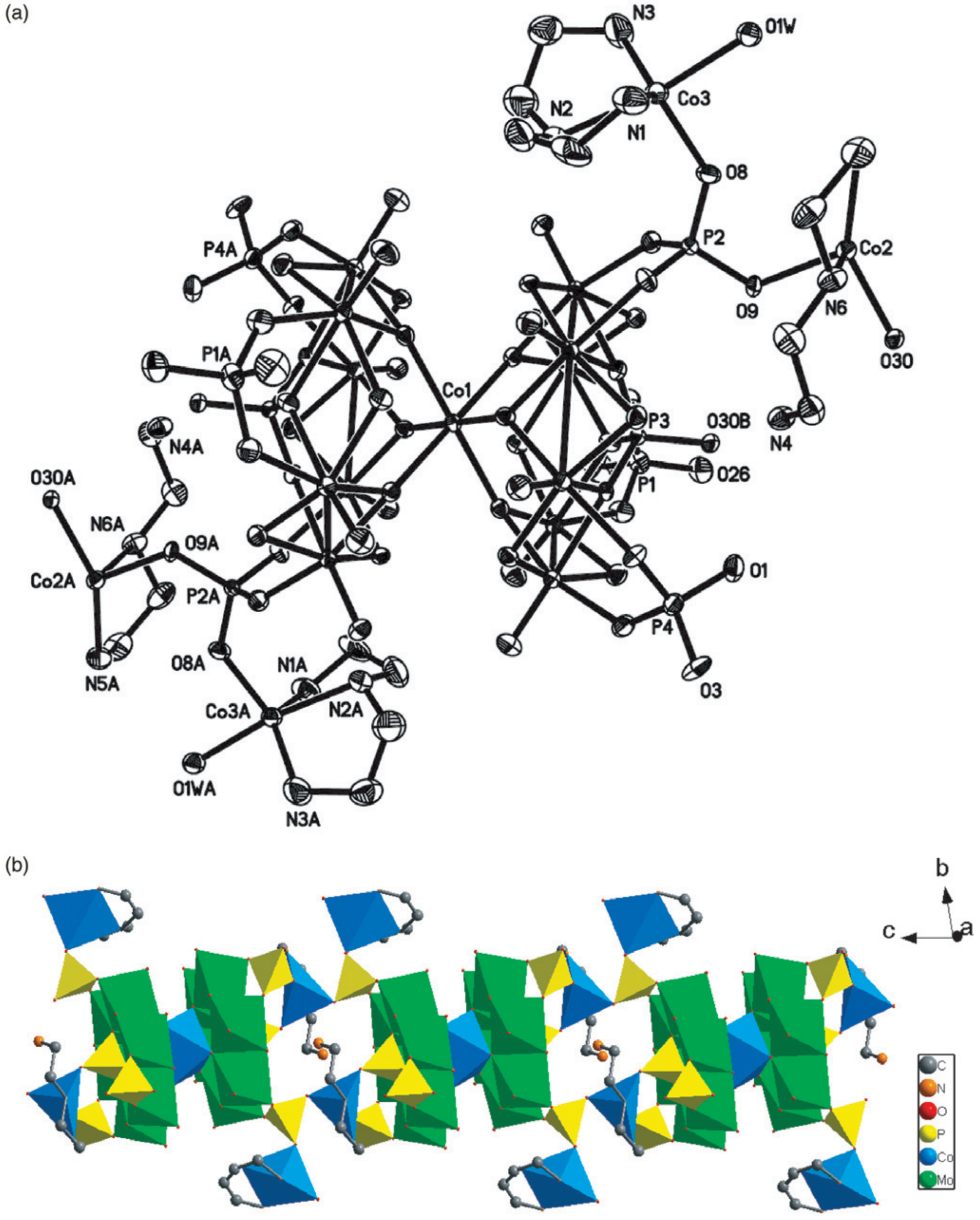

Figure 2. (a) Coordination environments of three types of Co atoms in **1**. (b) Polyhedral view of the infinite 1D chain of **1**.

3.3. *IR spectra*

The IR spectra of compounds **1** and **2** (figure S1) exhibit a broad band at 3261 cm^{-1} (**1**) and 3249 cm^{-1} (**2**) associated with the water molecules. The features at 1462, 1518, and 1599 cm^{-1} (**1**) and 1455, 1529, and 1618 cm^{-1} (**2**) are assigned to the dien molecules. The compounds also possess a strong band at 1027 cm^{-1} (**1**) and 1021 cm^{-1} (**2**) attributed to

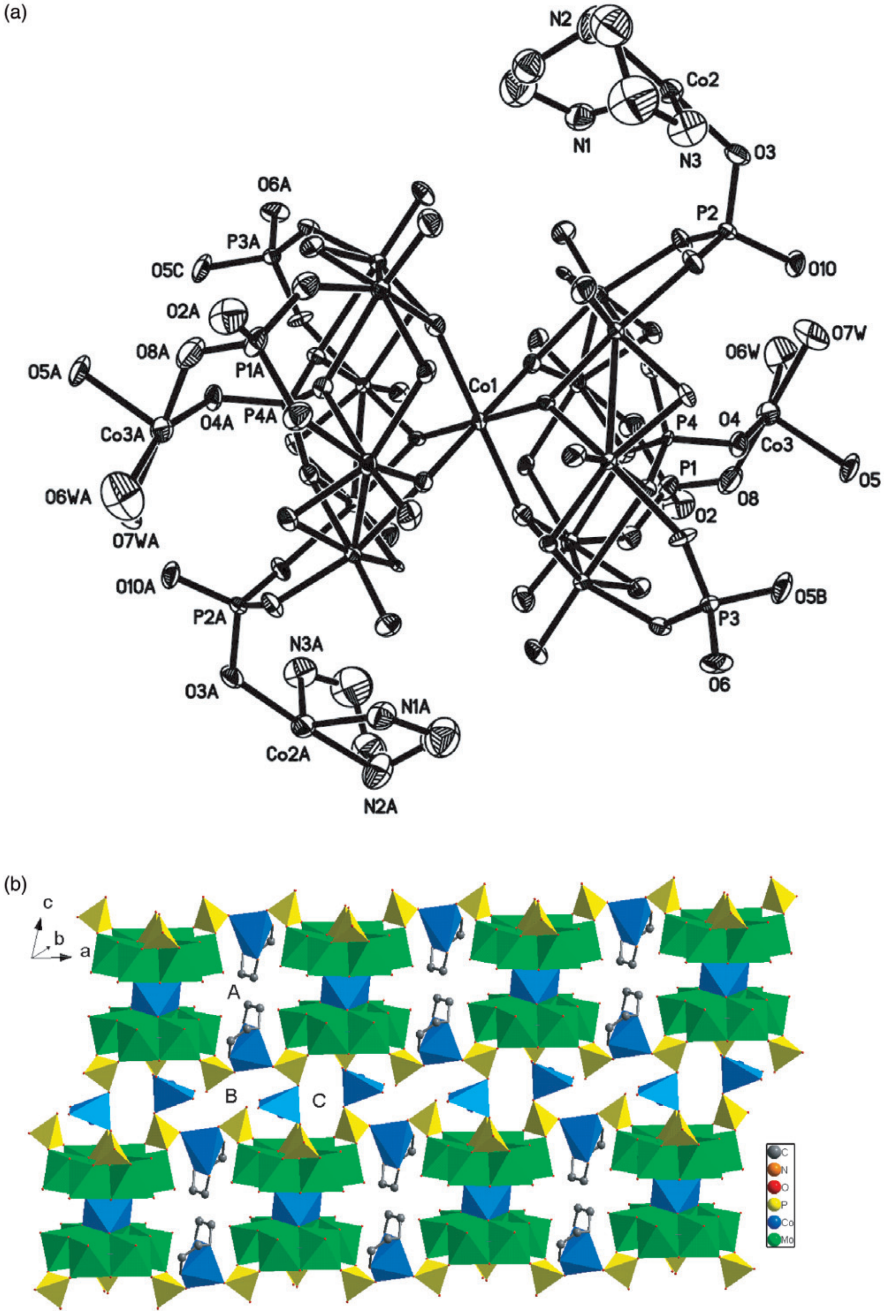

Figure 3. (a) Coordination environments of three types of Co atoms in **2**. (b) Polyhedral view of the 2D layer of **2**, showing three types of tunnels.

ν(P–O) and strong bands at 958, 743, and 683 (**1**) and 958, 743, and 683 (**2**) attributed to ν(Mo=O) and ν(Mo–O–Mo).

3.4. *Thermal analysis*

The TG curve of compound **1** (figure S2a) exhibits a total weight loss of 21.39% in the range of 82.17–618.1°C (Calcd 21.80%), in which, the weight loss of 3.55% in 82.17–264.01 corresponds to the loss of crystal and coordinated water molecules (Calcd 3.66%) and that of 17.84% in 264.01–618.1°C agrees with the loss of dien molecules (Calcd 18.14%).

The TG curve of compound **2** (figure S2b) exhibits two steps of weight loss. The first weight loss is 5.83% in the temperature range of 44.55–197.49°C, corresponding to the loss of crystal and coordinated water (Calcd 5.99%). The second weight loss is 12.65% from 259.65–600.76°C, assigned to the loss of dien molecules (Calcd 12.59%). The whole weight loss (18.58%) is in agreement with the calculated value (18.58%).

4. Electrochemical properties

4.1. *Apparatus*

A CHI 660 Electrochemical Workstation connected to a Digital-586 personal computer was used for control of the electrochemical measurements and for data collection. A conventional three-electrode system was used. The working electrode was $(Hdien)_2[Co(dien)]_2[Co(dien)(H_2O)]_2[CoMo_{12}O_{24}(HPO_4)_2(H_2PO_4)_2(PO_4)_4(OH)_6] \cdot 5H_2O$ bulk-modified carbon paste electrode (Mo_6P_4(**1**)-CPE) for compound **1**, and $(H_2dien)_2[Co(dien)]_2[Co(H_2O)_2]_2[CoMo_{12}O_{24}(HPO_4)_4(PO_4)_4(OH)_6] \cdot 7H_2O$ bulk-modified carbon paste electrode (Mo_6P_4 (**2**)-CPE) for compound **2**. A Ag–AgCl electrode was used as reference electrode and Pt gauze as a counter electrode. The Mo_6P_4-CPE was prepared following our earlier method [17].

4.2. *Results and discussions*

Since **1** and **2** were hydrothermally synthesized compounds and insoluble in most solvents, we fabricated Mo_6P_4-CPE following our earlier work [17, 18]. Figure 4 shows the voltammetric behaviors of Mo_6P_4 (**1**)-CPE (a) and Mo_6P_4 (**2**)-CPE (b) in 20 mL 0.1 M $Na_2SO_4 + 0.5M\ H_2SO_4$ aqueous solution at the scan rate of $50\,mV\,s^{-1}$. For Mo_6P_4 (**1**)-CPE, in the potential range +500 to 0 mV, two reversible redox peaks appear and the mean peak potentials $E_{1/2} = (E_{pa} + E_{pc})/2$ are 339 and 177 mV, respectively. Two redox peaks correspond to the two- and four-electron process, respectively. The voltammetric behavior of Mo_6P_4 (**2**)-CPE is similar, the mean peak potentials $E_{1/2} = (E_{pa} + E_{pc})/2$ are 344 and 176 mV, and two redox peaks correspond to the two- and four-electron process, respectively.

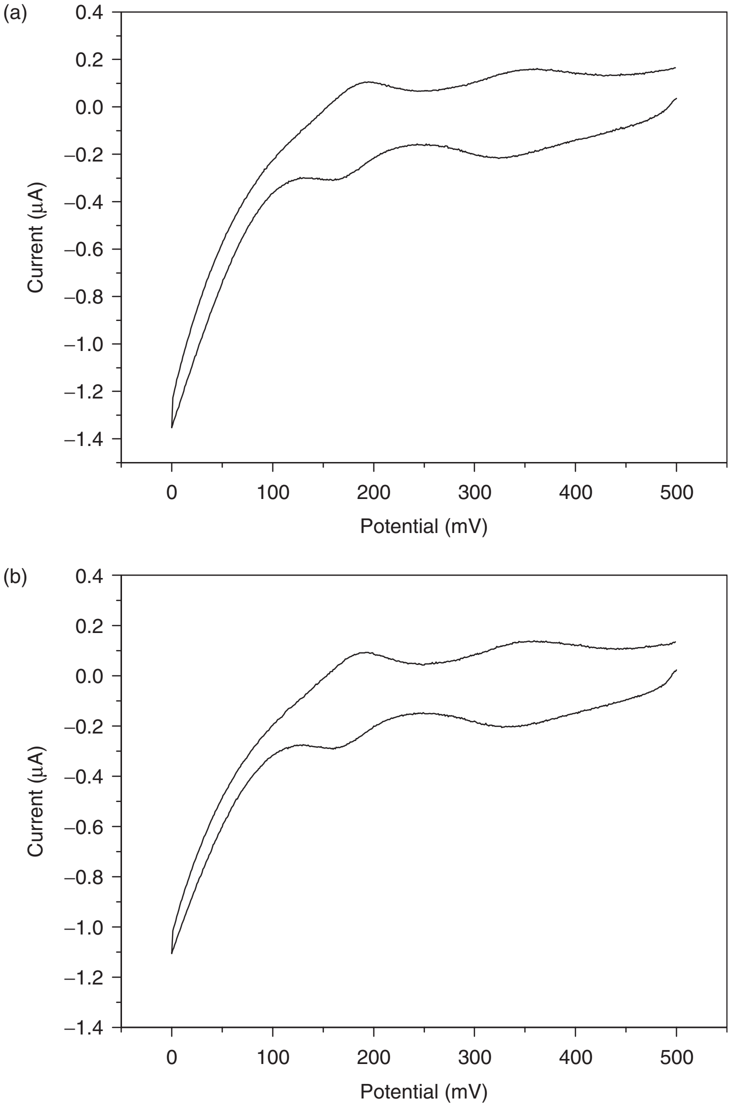

Figure 4. The cyclic voltammograms of Mo_6P_4 (**1**)-CPE (a) and Mo_6P_4 (**2**)-CPE (b) in 20 mL 0.1 M $Na_2SO_4 + 0.5$ M H_2SO_4 aqueous solution at the scan rate of $50\,mV\,s^{-1}$.

5. Magnetic properties of compound 2

The preliminary magnetic study of compound **2** was performed from 2 to 300 K at 10,000 Oe. The thermal variations of $\chi_m T$ and $1/\chi_m$ of compound **2** are displayed in figure 5. The $\chi_m T$ *versus* T plot decreases continuously from 16.83 emu K mol^{-1} at 300 K to reach 7.12 emu K mol^{-1} at 2 K. At 300 K, the $\chi_m T$ value is 16.83 emu K mol^{-1} (11.60 μB), which is approximately equal to that expected for the total value of five uncoupled $S = 3/2$ spins of Co^{2+} atoms and twelve uncoupled $S = 1/2$ spins of Mo^{5+} atoms (≈16.79 emu K mol^{-1} assuming $g(Co^{2+}) = g(Mo^{5+}) = 2.20$). Between 2 and 300 K, the magnetic behavior obeys the Curie–Weiss law [$\chi_m = C/(T - \theta)$] with

$C = 17.16\,\mathrm{emu\,K\,mol^{-1}}$ and $\theta = -9.59\,\mathrm{K}$. This behavior of $\chi_m T$ curve and Weiss temperature indicates that there exist antiferromagnetic interactions in **2**. However, in distorted octahedral or square-pyramidal Co(II) compounds we cannot assign exclusively to those interactions the thermal decrease of the magnetic effective moment or the observation of a negative Weiss temperature. Spin–orbit coupling is usually rather strong in these types of compounds and causes a qualitatively similar effect to an antiferromagnetic interaction. It is too difficult to fit the experimental magnetic data of this compound using a suitable theoretical model, and further studies on magnetic properties of similar systems are ongoing in our laboratory.

6. Conclusions

In summary, two inorganic–organic hybrid cobalt phosphomolybdates have been prepared under hydrothermal techniques. The [Co(dien)] complex is directly incorporated into the framework of **1** and **2** with a P–O–M (M = transition metal) mode, rarely seen in the $[Mo_6P_4]$ system. In addition, compounds **1** and **2** are cobalt molybdenum phosphates containing both square-pyramidal and octahedral transition metals, which possess 1D and 2D structures different from molybdenum phosphates containing $M[Mo_6P_4]_2$ as building blocks. Furthermore, the electrochemical properties of both compounds were studied via the method of bulk-modified carbon paste electrodes and the magnetic properties of compound **2** were reported. The incorporation of the cobalt cation into the molybdenum phosphate framework suggests that

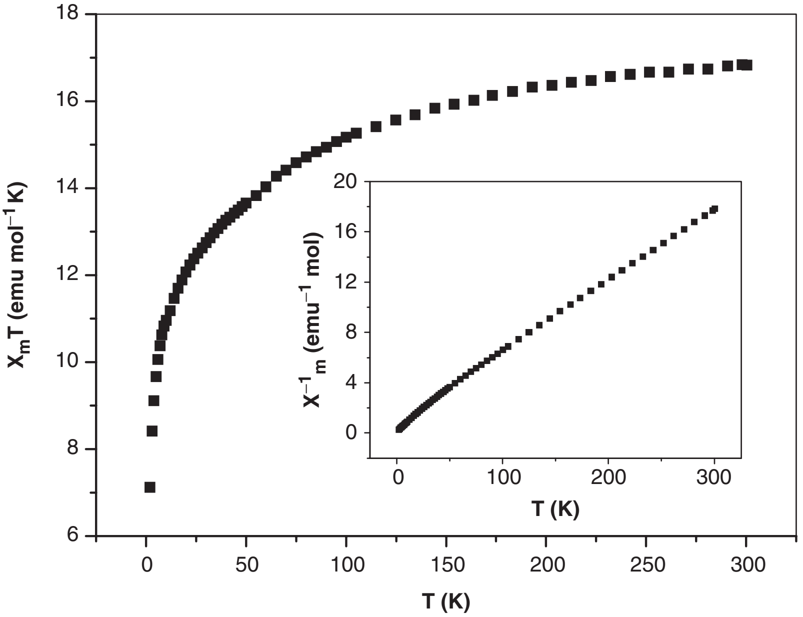

Figure 5. Thermal dependence of χ_m/T and $1/\chi_m$ for compound **2**.

analogous compounds can be derived from other first-row transition metals. More work in the field is underway.

Supplementary material

Crystallographic data for the structural analysis have been deposited with the Cambridge Crystallographic Data Center, CCDC reference number: 276317 for **1** and 276318 for **2**. These data can be obtained free of charge at www.ccdc.cam.ac.uk/conts/retrieving.html (or from the Cambridge Crystallographic Data Centre, 12, Union Road, Cambridge CB2 1EZ, UK; Fax: +44-1223/336-033; Email: deposit@ccdc.cam.ac.uk).

Acknowledgements

This work was financially supported by the National Natural Science Foundation of China (20371011).

References

[1] (a) O.M. Yaghi, H. Li. *J. Am. Chem. Soc.*, **118**, 295 (1996); (b) N.K. Raman, M.T. Aderson, C.F. Brinker. *Chem. Mater.*, **8**, 1683 (1996); (c) E. Canadell, J. Provost, A. Guesdon, M.M. Borel, A. Leclaire. *Chem. Mater.*, **9**, 68 (1997); (d) M.J. Zaworotko. *Angew. Chem., Int. Ed.*, **37**, 1211 (1998).

[2] (a) A.K. Cheetham, G. Férey, T. Loiseau. *Angew. Chem., Int. Ed.*, **38**, 3268 (1999); (b) Z. Shi, S.H. Feng, S. Gao, L.R. Zhang, G.Y. Yang, J. Hua. *Angew. Chem., Int. Ed.*, **39**, 2325 (2000); (c) Y. Lu, E.B. Wang, M. Yuan, G.Y. Luan, Y.G. Li. *J. Chem. Soc., Dalton Trans.*, 3029 (2002).

[3] (a) J.V. Smith. *Chem. Rev.*, **88**, 149 (1988); (b) K. Morgan, G. Gainsford, N. Milestone. *J. Chem. Soc., Chem. Commun.*, 425 (1995); (c) Y. Wang, J.H. Yu, M. Guo, R.R. Xu. *Angew. Chem., Int. Ed.*, **42**, 4089 (2003).

[4] (a) R.L. LaDuca Jr, R.S. Rarig Jr, J. Zubieta. *Inorg. Chem.*, **40**, 607 (2001); (b) C.M. Liu, Y.-L. Hou, J. Zhang, S. Gao. *Inorg. Chem.*, **41**, 1 (2002); (c) D.R. Xiao, Y. Xu, Y. Hou, E.B. Wang, S.T. Wang, Y.G. Li, L. Xu, C.W. Hu. *Eur. J. Inorg. Chem.*, 1385 (2004).

[5] (a) J.J. Lu, Y. Xu, N.K. Goh, L.S. Chia. *J. Chem. Soc., Chem. Commun.*, 2733 (1998); (b) L.J. Zhang, X.L. Zhao, J.Q. Xu, T.G. Wang. *J. Chem. Soc., Dalton Trans.*, 3275 (2002); (c) A. Dolbecq, P. Mialane, L. Lisnard, J. Marrot, F. Sécheresse. *Chem. Eur. J.* **9**, 2914 (2003); (d) A. Tripathi, T. Hughbanks, A. Clearfield. *J. Am. Chem. Soc.*, **125**, 10528 (2003).

[6] (a) S.T. Zheng, J. Zhang, G.Y. Yang. *Inorg. Chem.*, **44**, 2426 (2005); (b) M.I. Khan, E. Yohannes, R.J. Doedens. *Inorg. Chem.*, **42**, 3125 (2003); (c) B.Z. Lin, S.X. Liu. *J. Chem. Soc., Chem. Commun.*, 2126 (2002); (d) C.L. Pan, J.Q. Xu, G.H. Li, D.Q. Chu, T.G. Wang. *Eur. J. Inorg. Chem.*, 1514 (2003).

[7] R.C. Haushalter, L.A. Mundi. *Chem. Mater.*, **4**, 31 (1992).

[8] (a) S.T. Wang, E.B. Wang, Y. Hou, Y.G. Li, L. Wang, M. Yuan, C.W. Hu. *Trans. Met. Chem.*, **28**, 616 (2003); (b) L. Xu, Y.Q. Sun, E.B. Wang, E.H. Shen, Z.R. Liu, C.W. Hu. *New. J. Chem.*, **23**, 533 (1999); (c) C. du Peloux, P. Mialane, A. Dolbecq, J. Marrot, E. Rivière, F. Sécheresse. *J. Mater. Chem.*, **11**, 3392 (2001); (d) L.A. Meyer, R.C. Haushalter. *Inorg. Chem.*, **32**, 1579 (1993); (e) A. Leclaire, C. Biot, H. Rebbah, M.M. Borel, B. Raveau. *J. Mater. Chem.*, **8**, 439 (1998).

[9] Y.H. Sun, X.B. Cui, J.Q. Xu, L. Ye, Y. Li, J. Lu, H. Ding, H.Y. Bie. *J. Sol. State Chem.*, **177**, 1811 (2004).

[10] L. Xu, Y.Q. Sun, E.B. Wang, E.-H. Shen, Z.R. Liu, C.W. Hu. *J. Sol. State Chem.*, **146**, 533 (1999).

[11] X. He, P. Zhang, T.Y. Song, Z.C. Mu, J.H. Yu, Y. Wang, J.N. Xu. *Polyhedron*, **23**, 2153 (2004).

[12] (a) Y.S. Zhou, L.J. Zhang, H.K. Fun. *New. J. Chem.*, **25**, 1342 (2001); (b) Y.S. Zhou, L.J. Zhang, X.Z. You, S. Natarajan. *J. Sol. State Chem.*, **159**, 209 (2001).

[13] (a) M. Yuan, E.B. Wang, Y. Lu, Y.G. Li, C.W. Hu, N.H. Hu, H.Q. Jia. *Inorg. Chem. Commun.*, **5**, 505 (2002); (b) M. Yuan, E.B. Wang, Y. Lu, Y.G. Li, C.W. Hu, N.H. Hu, H.Q. Jia. *J. Solid State Chem.*, **170**, 192 (2003); (c) R.D. Huang, F.C. Liu, Y.G. Li, M. Yuan, E.B. Wang, G.J.H. De, C.W. Hu, N.H. Hu, H.Q. Jia. *Inorg. Chim. Acta*, **349**, 85 (2003); (d) H.X. Guo, S.X. Liu. *J. Mol. Struct.*, **741**, 229 (2005); (e) H.X. Guo, S.X. Liu. *Inorg. Chem. Commun.*, **7**, 1217 (2004); (f) H.X. Guo, S.X. Liu. *J. Mol. Struct.*, **751**, 156 (2005).

[14] (a) G.M. Sheldrick. *SHELX 97, Program for Crystal Structures Refinement*, University of Göttingen, Germany (1997); (b) G.M. Sheldrick. *SHELX 97, Program for Crystal Structures Solution*, University of Göttingen, Germany (1997).

[15] R.C. Haushalter, F.W. Lai. *Inorg. Chem.*, **28**, 2904 (1989).

[16] I.D. Brown, D. Altermatt. *Acta Cryst.*, **B41**, 244 (1985).

[17] (a) X.L. Wang, E.B. Wang, Y. Lan, C.W. Hu. *Electroanalysid*, **14**, 1116 (2002); (b) X.L. Wang, Z.-H. Kang, E.B. Wang, C.W. Hu. *Mater. Lett.*, **56**, 393 (2002).

[18] L.Y. Duan, F.C. Liu, X.L. Wang, E.B. Wang, C. Qin, Y.G. Li, X.L. Wang, C.W. Hu. *J. Mol. Struct.*, **705**, 15 (2004).

[19] C.M. Liu, D.Q. Zhang, M. Xiong, D.B. Zhu. *Chem. Commun.*, 1416 (2002).